The Bloch-Torrey Equation & Diffusion Imaging (DWI, DTI, q-Space Imaging)

Jennifer A. McNab, Ph.D.
Assistant Professor, Department of Radiology
Stanford University

The effect of diffusion on the magnetic resonance signal was first noted by Hahn in 1950 [1] and later by Carr and Purcell in 1954 [2] . In 1956 Torrey incorporated these effects into the Bloch Equations, creating the so-called Bloch-Torrey Equation [3]:

$$\frac{d\mathbf{M}}{dt} = \gamma(\mathbf{M} \times \mathbf{B_0}) + \begin{pmatrix} \frac{M_x}{T_2} \\ \frac{M_y}{T_2} \\ \frac{M_0 - M_z}{T_1} \end{pmatrix} + D\nabla^2\mathbf{M} \quad (1)$$

Here, $\mathbf{M}$ is the magnetization of an excited sample placed in a static magnetic field $\mathbf{B_0}$, γ is the gyromagnetic ratio, M_x, M_y, M_z are the components of magnetization in the x, y and z directions, M_0 is the magnetization at thermal equilibrium, T_1 and T_2 are the longitudinal and transverse relaxation times and D is the diffusion coefficient. The first two terms of Equation 1 are the original Bloch Equation [4]. The third term of Equation 1 was added by Torrey. The solution to the Bloch-Torrey equation (Equation 1) for magnetization in the transverse plane ($M_{xy} = M_x + iM_y$) following a 90° pulse is given by,

$$M_{xy} = M_0 e^{-\frac{t}{T_2}} e^{-bD} \quad (2)$$

which is analogous to the well-known solution for a spin-echo experiment with an additional multiplicative factor $exp(-bD)$. b describes the diffusion sensitizing magnetic gradient amplitude (G) and timing and is given by,

$$b = \gamma^2 \int_0^{TE} (\int_0^t G(t')dt')^2 dt \quad (3)$$

The use of a balanced bipolar magnetic gradient (Figure 1a) for the measurement of diffusion was developed by Stejskal and Tanner [5]. The underlying principle of the balanced bipolar gradient pulse is that the first gradient lobe will impart a spatially-dependent phase to each excited spin. For stationary spins, the second gradient lobe will reverse the phase introduced by the first gradient lobe and hence the bipolar gradient will have no net effect. Each proton that experiences random diffusive displacements between the application of the two gradient pulses will acquire a phase offset proportional to the magnitude of the displacements. The result is a phase dispersion proportional to the spread of positions, which in turn attenuates the signal exponentially according the amplitudes and timing of the gradients (b) and the diffusion coefficient (D). For a Stejskal-Tanner bipolar pair pulses shown in Figure 1a, b (as defined in Equation 3) is:

$$b = (\gamma G \delta)^2 (\Delta - \frac{\delta}{3}) \quad (4)$$

where G is the gradient strength in mT/m, δ is the duration of a single lobe and Δ is time between the start of the first and second lobes. The diffusion coefficient (D) along any direction can therefore be measured by comparing the MRI signal S with and without diffusion-weighting gradients in the following manner:

$$S(b) = M_0 e^{-t/T_2} e^{-bD} \quad (5)$$

$$S(b=0) = M_0 e^{-t/T_2} \quad (6)$$

$$D = \frac{ln\frac{S(b)}{S(b=0)}}{-b} \quad (7)$$

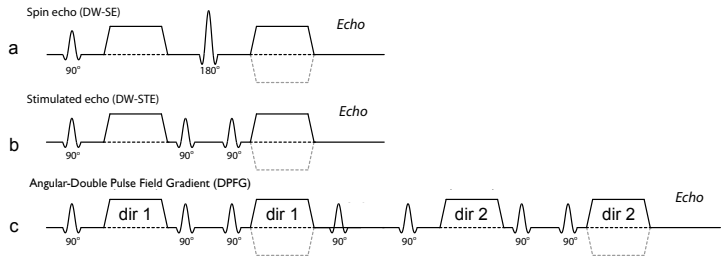

Figure 1: Pulse sequence diagrams for a) diffusion-weighted spin echo, b) diffusion-weighted stimulated echo and c) angular-double pulsed field gradient diffusion imaging.

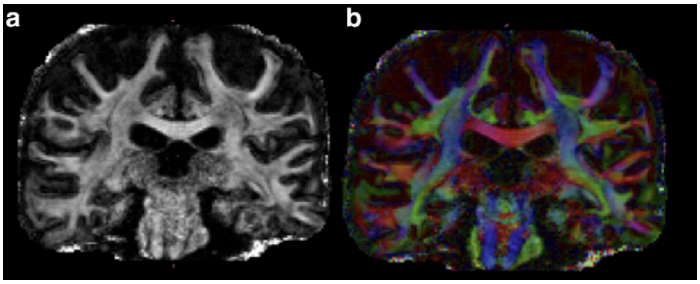

Figure 2: Diffusion tensor images in the coronal plane: a) fractional anisotropy and b) directionally-encoded colour (DEC) with red:blue:green representing L-R:S-I:A-P.

Diffusion Tensor Imaging

In neural tissue, water diffuses more rapidly along the length of white matter fibres than in perpendicular directions resulting in an unequal (anisotropic) spread of water molecule positions which is well-described by a tensor formalism. Mathematically the diffusion tensor (D), is a symmetric 3×3 co-variance matrix with six unique elements:

$$\mathbf{D} = \begin{pmatrix} D_{xx} & D_{xy} & D_{xz} \\ D_{xy} & D_{yy} & D_{yz} \\ D_{xz} & D_{yz} & D_{zz} \end{pmatrix} \tag{8}$$

To measure the diffusion tensor, ADC maps must be acquired with the diffusion sensitizing gradients applied along at least six non-collinear directions [6]. An excellent introduction to diffusion tensor mathematics is a three part series of manuscripts written by Peter Kingsley [7,8,9]. For a regular, parallel arrangement of fibres the rate of diffusion along the fibres is about ten times larger than in perpendicular directions [10]. By determining the direction of maximum diffusivity (the principal eigenvector of the diffusion tensor), the orientation of white matter tracts and hence anatomical connections can be inferred [6,10]. This type of orientational information is commonly displayed using directionally encoded colour (DEC) maps [10] (Fig. 2b). The diffusion tensor also yields several useful metrics for characterizing diffusion in brain tissue including fractional anisotropy (FA) (Fig. 2a), the trace of the diffusion tensor and mean diffusivity <D> :

$$FA = \sqrt{\frac{3}{2}\frac{\sum_{i=1,2,3}(\lambda_i - \bar{\lambda})^2}{\sum_{i=1,2,3}\lambda_i^2}} \tag{9}$$

$$Trace(D) = (\lambda_1 + \lambda_2 + \lambda_3) \tag{10}$$

$$< D >= \frac{\lambda_1 + \lambda_2 + \lambda_3}{3} \tag{11}$$

where λ_1,λ_2,λ_3 represent the eigenvalues of the diffusion tensor. While diffusion tensor imaging has achieved widespread utility in the neuroimaging community, the tensor model fails to characterize tissue microstructure when non-Gaussian diffusion effects are present. For example, when two or more fibre bundles cross within a voxel, the diffusion tensor erroneously detects isotropic diffusion. A second example of non-Gaussian diffusion effects that confound the interpretation of the diffusion tensor are tissue boundary effects (i.e. patterns of diffusion caused by water molecules bouncing off of membranes or macromolecules) which can be observed at long diffusion times and/or when strong diffusion-encoding gradients are used. Crossing fibre and/or multi-exponential diffusion models can be used to characterize these non-Gaussian effects but an alternative approach is to use a model-free method known as q-space imaging.

Q-space Imaging

Q-space imaging methods require sampling of a range of q-values, where a q-value is proportional to the diffusion-encoding gradient area.

$$\mathbf{q} = \frac{\gamma}{2\pi}\int_0^{\delta} \mathbf{G}(t)dt \tag{12}$$

Using this q-space formalism, the signal (E) at a given $\mathbf{q}$ and diffusion time (Δ) is given by:

$$E(\mathbf{q},\Delta) = \int P(\mathbf{r},\Delta)exp(-i2\pi\mathbf{q}\cdot\mathbf{r})d\mathbf{r} \tag{13}$$

where $P(\mathbf{r}, \Delta)$ is the spin displacement probability distribution function (*pdf*) or rather the probability that a molecule has been displaced by $\mathbf{r}$ in a time Δ. Therefore, the spin displacement *pdf* may be extracted by taking the inverse Fourier Transform of the signal attenuation at multiple q-values. Just as $1/k_{max}$ determines the spatial resolution of an MR image, $1/q_{max}$ determines the "diffusion-resolution" or rather the ability to resolve differences in the mean displacements of water molecules. Similarly, 1/Δq determines the field-of-view of the spin displacement *pdf*.

Diffusion Spectrum Imaging (DSI): If multiple q-values are acquired along multiple diffusion-encoding orientations an estimation of the 3D spin displacement *pdf* is possible and this is the basis of Diffusion Spectrum Imaging (DSI) [11,12] (Fig. 3). Since no model is assumed, 3D spin displacement *pdfs* can, given adequate q_{max}, Δ, and sufficient q-space sampling (angular resolution), detect any 3D diffusion pattern. In the case of a single fibre orientation within a voxel, and for the large displacement (large r) and small q regime, the spin displacement probability distribution measured by q-space MRI is the same as the 3D Gaussian displacement distribution assumed in DTI [13].

DSI has intense sampling requirements (e.g. even an 8x8x8 grid sampling q_x,q_y,q_z space requires 512 measurements). These high sampling requirements motivated the development of q-ball imaging [14] which provides an approximation of DSI spin-displacement *pdf* using data acquired on only a single shell of q-space rather than a the full q-space grid.

Both DSI and q-ball require high q-values to resolve more detailed diffusion patterns and this places high demands on the encoding gradients since the longer it takes to play out the diffusion encoding the more signal is lost due to T_2 decay and the lower the sensitivity of the acquisition. For these reasons, DSI acquisitions have traditionally been difficult to achieve in a feasible time for an *in vivo* human scan and tended to use larger voxels compared to other diffusion imaging techniques (e.g. 3 mm isotropic) in order to gain sufficient sensitivity levels. Recent advances in engineering stronger gradients (100-300 mT/m compared to ~40mT/m) for human scanners such as those built for the NIH Blueprint Human Connectome Project [15] are rapidly changing this paradigm and rendering q-space imaging methods clinically feasible for the first time.

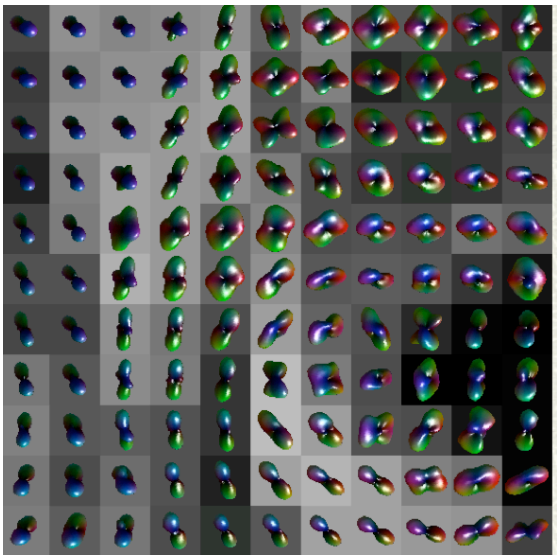

Figure 3: Examples of orientation distribution functions generated by diffusion spectrum imaging.

Axon Diameter Distribution Mapping: A different genre of q-space imaging focuses on sampling temporal q-space rather than spatial q-space (i.e. acquire multiple q-values at multiple diffusion times). If sufficiently high q-values and long diffusion times are acquired, it is possible to extract information about the size of restricted compartments(e.g axons) based on theoretical models of the "diffusion diffraction" patterns that they will generate. In the simplest version of this technique, diffusion is only encoded along the orientation that is orthogonal to the long axis of the white matter tract of interest [16, 17, 18, 19]. The q-space data is fit to a model of water diffusion within and between a densely packed array of cylinders (axons) of varying sizes. In this way a **probability density distribution of a range of axon sizes** can be estimated. Since long diffusion times are needed for this method, a diffusion-weighted stimulated-echo pulse sequence

(Fig.1b) is sometimes used to reduce signal decay during the time between the two diffusion-encoding gradients. Similar to DSI the high sampling demands and the need for high-q values and long diffusion times make it difficult to achieve clinically feasible scan times with good sensitivity. Therefore, q-space compartment mapping techniques have largely been limited to *in vitro* [16, 17, 18] and pre-clinical [19] models because the necessary encoding gradients have only been available on small bore MRI scanners. Development of similar techniques that can be performed at clinical gradient strengths is an active area of research [20,21].

Angular-Double Pulsed Field Gradient (DPFG) Imaging: Angular-DPFG imaging [22,23] has both a temporal and spatial component to its q-space sampling. Angular-DPFG imaging sensitizes the MRI signal first to diffusion along one orientation and then after a specified time, along a second different orientation (Fig. 1c). The angle between the first diffusion-encoding orientation and the second diffusion-encoding orientation is then gradually incremented from 0° to 180°. In this way, angular-DPFG imaging is able to resolve the **shape of restricted compartments** even if they are not coherently organized.

References:

1. E L Hahn. Spin echoes. *Physical Review*, 80:580–594 (1950).
2. H Y Carr and E M Purcell. Effects of diffusion on free precession in nuclear magnetic resonance. *Physical Review*, 94:630–638 (1954).
3. H C Torrey. Bloch equations with diffusion terms. *Physical Review*, 104:563–565 (1956).
4. F Bloch. Nuclear induction. *Physics Review*, 70:460–470 (1946).
5. E O Stejskal and J E Tanner. Spin-diffusion measurements:spin echoes in the presence of a time-dependent field gradient. *Journal of Chemical Physics*, 42:288–292 (1965).
6. P J Basser, J Mattiello, and D Le Bihan. MR diffusion tensor spectroscopy and imaging. *Biophysics Journal*, 66:259–267 (1994).
7. Kingsley PB. Introduction to Diffusion Tensor Imaging Mathematics Part I. Tensors, Rotations, and Eigenvectors, *Concepts in Magnetic Resonance Part A* 28A: 101-122 (2006).
8. Kingsley PB. Introduction to Diffusion Tensor Imaging Mathematics Part II. Anisotropy, Diffusion-Weighting Factors, and Gradient Encoding Schemes, *Concepts in Magnetic Resonance Part A* 28A: 123-154 (2006).
9. Kingsley PB. Introduction to Diffusion Tensor Imaging Mathematics Part III. Tensor Calculation, Noise Simulations and Optimization, *Concepts in Magnetic Resonance Part A* 28A: 155-179 (2006).
10. C Pierpaoli and P J Basser.Toward a quantitative assessment of diffusion anisotropy. *Magnetic Resonance in Medicine*, 36:893–906 (1996).
11. Callaghan PT, Eccles CD, Xia Y. NMR microscopy of dynamic displacements - k-spaced and q-space imaging, *J. Phys. E: Sci. Instrum.* 21:820-822 (1988).
12. Wedeen VJ, Hagmann P, Tseng WY, Reese TG, Weisskoff RM. Mapping complex tissue architecture with diffusion spectrum magnetic resonance imaging, *Magnetic Resonance in Medicine* 54(6):1377-86 (2005).
13. Basser PJ. Relationships Between Diffusion Tensor and q-Space MRI. *Magnetic Resonance in Medicine* 47: 392-397 (2002).
14. Tuch D. Q-Ball Imaging, *Magnetic Resonance in Medicine* 52:1358-1372 (2004).
15. Kimmlingen R, Eberlein E, Dietz P, Kreher S, et. al. Concept and Realization of High Strength Gradients for the Human Connectome Project. *Proceedings of the Annual Meeting of the International Society for Magnetic Resonance in Medicine*, 20 (2012).
16. Stanisz GJ, Szafer A, Wright GA, Henkelman RM. An analytical model of restricted diffusion in bovine optic nerve. *Magnetic Resonance in Medicine*, 37:103-111 (1997)
17. Assaf Y, Blumenfeld-Katzir T, et. al. AxCaliber: a method for measuring axon diameter distribution from diffusion MRI, *Magnetic Resonance in Medicine*, 59:1347-54. (2008).
17. Ong HH, Wehrli FW. Quantifying axon diameter and intra-cellular volume fraction in excised mouse spinal cord with q-space imaging, *NeuroImage* 51:1360-6 (2010)
18. Barazany B, Basser PJ, Assaf Y. In vivo measurement of axon diameter distribution in the corpus callosum of rat brain, *Brain* 132, 1210-1220 (2009).
19. Alexander DC, Hubbard PL, Hall MG, Moore EA, Ptito M, Parker GJ and Dyrby T. Orientationally invariant indices of axon diameter and density from diffusion MRI. *NeuroImage* 52:1374-1389 (2010).
20. Zhang H, Hubbard PL, Parker GJM, Alexander DC. Axon Diameter Mapping in the Presence of Orientation Dispersion with Diffusion MRI, *NeuroImage* 56:1301-1315 (2011).
21. Mitra PP. Multiple wave-vector extensions of the NMR pulsed-field-gradient spin-echo diffusion measurement, *Phys Rev B Condens Matter* 51:15074-15078 (1995).
22. Shemesh N, Cohen Y. Microscopic and compartment shape anisotropies in gray and white matter revealed by angular bipolar double-PFG MR. *Magnetic Resonance in Medicine*, 65, 1216-27 (2011).